Human Molecular Genetics, 2010, Vol. 19, No. 22 ***4437–4452***
doi:10.1093/hmg/ddq370
Advance Access published on September 2, 2010

Dissecting the role of the mitochondrial chaperone mortalin in Parkinson's disease: functional impact of disease-related variants on mitochondrial homeostasis

Lena F. Burbulla[1,2,3], Carina Schelling[1,2], Hiroki Kato[4], Doron Rapaport[4], Dirk Woitalla[7], Carola Schiesling[1,2], Claudia Schulte[1,2], Manu Sharma[1,2], Thomas Illig[8], Peter Bauer[5], Stephan Jung[6], Alfred Nordheim[6], Ludger Schöls[1,2], Olaf Riess[5] and Rejko Krüger[1,2,*]

[1]DZNE, German Center for Neurodegenerative Diseases, Tübingen, Germany, [2]Department of Neurodegenerative Diseases, Hertie-Institute for Clinical Brain Research, [3]Graduate School of Cellular & Molecular Neuroscience, [4]Interfaculty Institute for Biochemistry, [5]Medical Genetics and [6]Proteome Center Tübingen, Interfaculty Institute for Cell Biology, University of Tübingen, Tübingen, Germany and [7]Department of Neurology, St Josef-Hospital, Ruhr-University Bochum, Bochum, Germany and [8]Institute of Epidemiology, Helmholtz Zentrum München, German Research Center for Environmental Health, Neuherberg, Germany

Received July 21, 2010; Revised August 20, 2010; Accepted August 26, 2010

The mitochondrial chaperone mortalin has been linked to neurodegeneration in Parkinson's disease (PD) based on reduced protein levels in affected brain regions of PD patients and its interaction with the PD-associated protein DJ-1. Recently, two amino acid exchanges in the ATPase domain (R126W) and the substrate-binding domain (P509S) of mortalin were identified in Spanish PD patients. Here, we identified a separate and novel variant (A476T) in the substrate-binding domain of mortalin in German PD patients. To define a potential role as a susceptibility factor in PD, we characterized the functions of all three variants in different cellular models. *In vitro* import assays revealed normal targeting of all mortalin variants. In neuronal and non-neuronal human cell lines, the disease-associated variants caused a mitochondrial phenotype of increased reactive oxygen species and reduced mitochondrial membrane potential, which were exacerbated upon proteolytic stress. These functional impairments correspond with characteristic alterations of the mitochondrial network in cells overexpressing mutant mortalin compared with wild-type (wt), which were confirmed in fibroblasts from a carrier of the A476T variant. In line with a loss of function hypothesis, knockdown of mortalin in human cells caused impaired mitochondrial function that was rescued by wt mortalin, but not by the variants. Our genetic and functional studies of novel disease-associated variants in the *mortalin* gene define a loss of mortalin function, which causes impaired mitochondrial function and dynamics. Our results support the role of this mitochondrial chaperone in neurodegeneration and underscore the concept of impaired mitochondrial protein quality control in PD.

INTRODUCTION

Parkinson's disease (PD) is the second most common neurodegenerative disorder after Alzheimer's disease. Although for the majority of patients the underlying cause of the disease is still unknown, existing data suggest that genetic susceptibility factors acting together with environmental risk factors are contributing to the sporadic form of the disease. Following

*To whom correspondence should be addressed at: Laboratory of Functional Neurogenomics, Center of Neurology, Hertie-Institute for Clinical Brain Research, University of Tübingen, Hoppe-Seyler-Str. 3, 72076 Tübingen, Germany. Tel: +49 70712982141; Fax: +49 7071295260; Email: rejko.krueger@uni-tuebingen.de

linkage studies in rare familial forms of PD and the screening of large samples of sporadic PD patients, to date, 16 genetic disease loci have been identified including several genes that allowed the first insight into molecular pathways leading to neurodegeneration (1,2). The identification of PD patients with variants in nuclear encoded mitochondrial proteins was the first genetic support for various biochemical findings that had previously implicated impaired mitochondrial function in PD pathogenesis (3–5).

A specific and selective loss of mitochondrial complex I activity in the substantia nigra of PD patients reflects an important role of mitochondrial pathology in PD (6). Furthermore, mitochondrial homeostasis plays a crucial role in aging and programmed cell death. Nevertheless, the intramitochondrial signaling pathways involved in cellular stress response and initiation of cell death mechanisms are currently poorly understood.

Variants in the *DJ-1* gene have established an important link between mitochondrial impairment and the pathogenesis of PD. Oxidation of DJ-1 and its subsequent translocation to the mitochondrion were identified as crucial for the maintenance of mitochondrial homeostasis (7–9). *DJ-1* encodes a mitochondrial protein that acts as a sensor of cellular oxidative stress and exerts a crucial role in protecting cells against stress-induced cell death (8). Known loss-of-function DJ-1 variants decrease the protective capacities against neuronal cell death and can play a critical role in the susceptibility to neurodegeneration (10,11).

Recently, the mitochondrial heat shock protein mortalin (also known as GRP75, mthsp70 or PBP74) was identified as a novel mitochondrial DJ-1-interacting protein, also involved in the oxidative stress response (12,13). Mortalin is a 679 amino acid protein that has been found in multiple subcellular localizations such as the endoplasmic reticulum, cytoplasmic vesicles and the cytosol (14,15). However, the majority of mortalin is located within the mitochondrial matrix. The protein reaches this location after its import via the translocases of the mitochondrial outer and inner membranes (16,17). Moreover, mortalin also takes an active role in the import of other proteins via the translocases of the mitochondrial inner membrane channels. It has been identified as the only ATPase component of the preprotein mitochondrial import complex and is therefore essential for effective import of nuclear encoded proteins into mitochondria (18,19). Interestingly, in the brain, mortalin primarily localizes to neurons, but is observed in glial cells upon pathological activation (20–22).

As a lifespan-regulating protein and a member of the Hsp70 family of chaperones, mortalin is also involved in the regulation of cellular senescence and immortalization. Lifespan-regulating proteins directly affect mitochondrial function, including energy metabolism and reactive oxygen species (ROS) production (23,24). Importantly, stress response and aging are recognized as major risk factors for neurodegenerative diseases such as PD (23,25–27). Impaired mitochondrial function is critically linked to imbalanced dynamic fusion and fission events of mitochondria and to energetic depression, which may subsequently result in the activation of programmed cell death mechanisms. Overexpression of mortalin leads to an extended lifespan in nematodes and in human cells (28,29). On the other hand, it serves as a major target for oxidation and was shown to be involved in aging of the human brain, including PD (30). Since mortalin interacts with many proteins (31), its modifications in response to oxidation-related stress and damage are likely to generate pleiotropic effects (32).

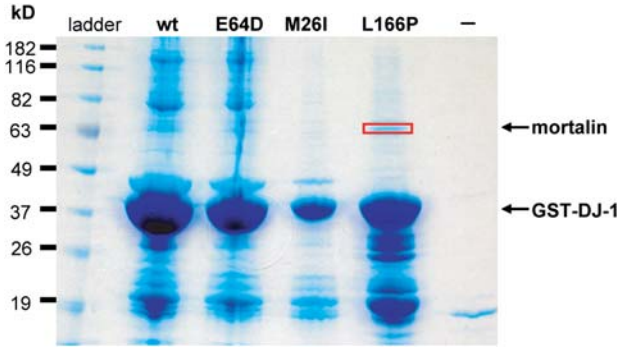

Figure 1. Identification of mortalin as a DJ-1-interacting protein using a proteomic approach. We performed a GST pull-down assay on lysates from dopaminergic neuroblastoma cells (SK-N-BE) with recombinant DJ-1-GST fusion proteins including wt protein and three known point variants (M26I, E64D and L166P). Samples were analyzed by 8% SDS–PAGE and stained with Coomassie. The first lane represents a protein marker with kilodalton weights indicated on the left followed by the different DJ-1 constructs used as a bait (lane 2: wt DJ-1; lane 3: E64D mutant DJ-1; lane 4: M26I mutant DJ-1; lane 5: L166P mutant DJ-1). Subsequent LC-ESI-MS/MS analyses identified mortalin as a specific binding partner of DJ-1 (red box).

Recently, the following observations suggested a role for mortalin in PD pathogenesis: (i) mortalin binds the PD-associated gene *DJ-1*, (ii) it plays an important role in the maintenance of mitochondrial homeostasis as critically related to neurodegeneration and (iii) coding variants in the *mortalin* gene in PD patients have been identified. Considering these associations, we first performed a mutational screening in a large sample of German PD patients, followed by functional mutation analyses including all PD-associated mortalin variants. Our observation that the loss of mortalin performance can cause impaired mitochondrial function and morphology provides a mechanism for the pathogenic role of mortalin in PD.

RESULTS

Unbiased proteomic approach identifies mortalin as a binding partner of DJ-1

Using a glutathion *S*-transferase (GST) pull-down assay with recombinant GST-tagged DJ-1 protein, we screened for DJ-1-interacting proteins in lysates from human dopaminergic neuroblastoma cells (SK-N-BE). Selected protein bands on a Coomassie gel were in-gel-digested and submitted to LC-ESI-MS/MS analysis. In comparison with publicly available databases, we identified mortalin as a DJ-1-interacting protein in lysates from human dopaminergic SK-N-BE cells (Fig. 1).

Processing mass spectrometry data by using OpenMS and Mascot search engines, we identified mortalin as a DJ-1-interacting protein, with a probability-based mowse score of 139 indicating a high degree of homology (33). This interaction was subsequently confirmed by co-immunoprecipitation of wild-type (wt) DJ-1-myc and mortalin-V5 in HEK293 cells (data not shown). Therefore, our results confirm previous studies using either a candidate approach or an alternative

Table 1. Frequency of the identified polymorphisms in the coding region of the *mortalin* gene in patients and controls

Polymorphism	Detection method	Patients	Controls
Ala81Ala (exon 4)	dHPLC, sequencing	2.1% (6/286)	2.6%[a]
Gln258Gln (exon 8)	dHPLC, sequencing	3.15% (9/286)	4.8%[a]
Lys316Lys (exon 9)	dHPLC, sequencing	54% (85/157)	42% (116/276)
Leu645Leu (exon 16)	dHPLC, sequencing	46% (129/279)	45% (85/191)

[a]http://www.ensembl.org/Homo_sapiens/Transcript/ProtVariations?db=core;g=ENSG00000113013;r=5:137918923-137939014;t=ENST00000297185.

proteomic approach, i.e. stable isotope labeling by amino acids in cell culture, to define the interaction between DJ-1 and the mitochondrial chaperone protein mortalin (12,13).

Identification of a novel mortalin variant in German PD patients

Initially, we performed a detailed mutational analysis of the coding region of the *mortalin* gene in a sample of 286 German PD patients (mean age: 65.1 ± 10.5 years; males: 51.9%, females: 48.1%). Using denaturating high-performance liquid chromatography (dHPLC) analysis of amplified PCR fragments for high-throughput mutational screening and subsequent direct sequencing, we were able to define sequence variations of German PD patients from that of a group of 290 healthy German controls. In total, we identified five sequence variations in the coding region of the *mortalin* gene. Most of them were silent base pair exchanges representing known polymorphisms without evidence of disease association (Table 1). However, a novel c.1426G>A variant in exon 12 was identified in one apparently sporadic PD patient, leading to an amino acid exchange from alanine to threonine in position 476 (Supplementary Material, Fig. S1A). The A476T variant is located in a highly conserved region of the protein sequence that forms part of the substrate-binding domain of the protein (Fig. 2A and B). This variant, which was identified in the heterozygous state in the carrier, was not present in 580 chromosomes of population and age-matched healthy controls.

Consequently, we screened an independent cohort of 1008 German PD patients (mean age of patients at onset 56.0 ± 12.1 years; males: 59.0%, females: 41.0%) and 1342 population-based matched controls (mean age of controls at examination 55.6 ± 11.7 years; males: 58.7%, females: 41.3%) for the identified novel variant in the German population and two recently identified *mortalin* variants from Spanish PD patients [c.376C>T and c.1525C>T; (34)]. The latter variants were each identified in individual Spanish PD patients and affect highly conserved regions of the protein, which was discovered by an interspecies comparison (Fig. 2C and D).

The variants identified in Spanish PD patients were absent in our cohorts, as all patients and controls were homozygous for the respective wt allele. The heterozygous A476T exchange was subsequently identified in four additional PD patients and six individuals from the population-based controls. Interestingly, four of the control individuals carrying the A476T variant

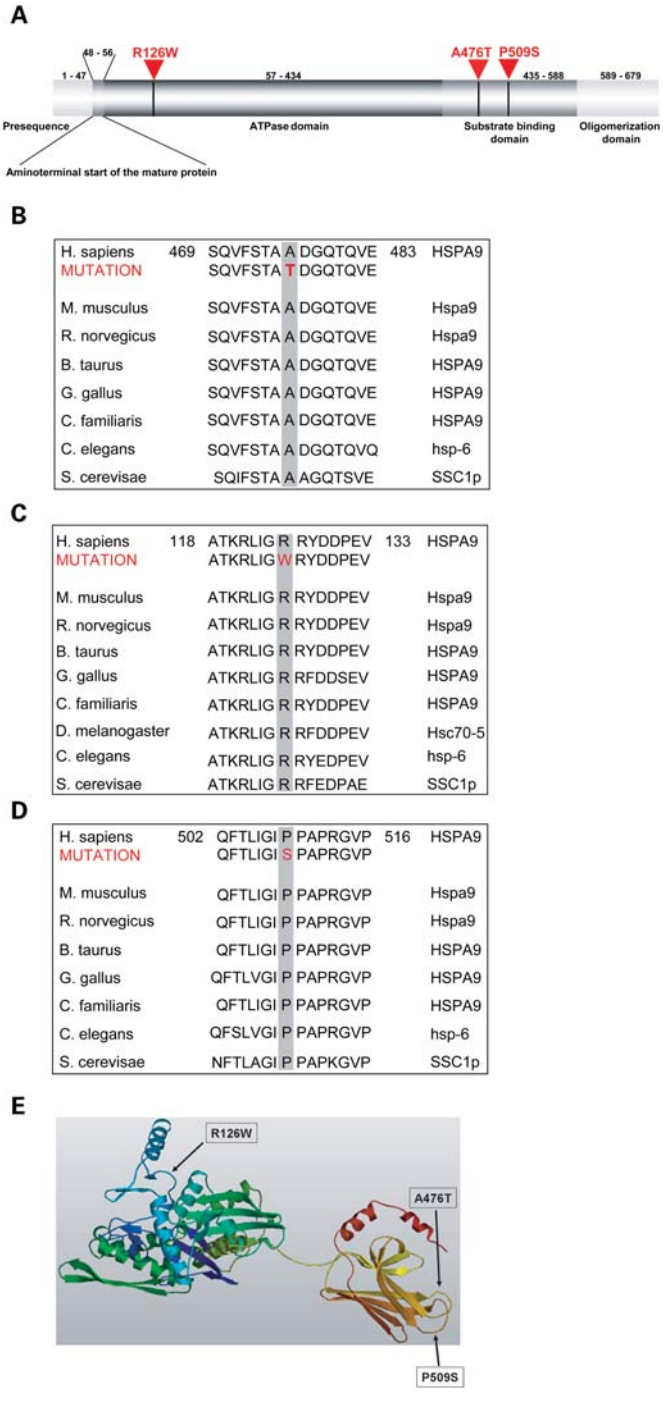

Figure 2. Localization, interspecies comparison and homology modeling of three novel mortalin variants. (**A**) A schematic diagram of the various protein domains of the mitochondrially targeted protein mortalin. The variants A476T and P509S are located in the substrate-binding domain, whereas the R126W variant affects the ATPase domain. All of the variants affect highly conserved regions of the protein. (**B**–**D**) An interspecies comparison of the amino acid sequence of the mortalin protein. (**E**) Homology modeling based on the predicted structure of mortalin as derived from the homology to *Geobacillus kaustophilus* HTA426 was assessed by SWISS-MODEL (http://swissmodel.expasy.org). The arrows indicate the sites of the variants.

were reported with previously defined extrapyramidal symptoms that did not fulfill the diagnosis of PD (mean age 72.6 ± 5.3 years), whereas the other two asymptomatic carriers of the A476T variant were significantly younger (mean age 44.5 ± 9.5 years). Collectively, this leads to a frequency of the A476T variant of 0.0069 in individuals with extrapyramidal symptoms and a frequency of 0.0012 in healthy controls. We speculated that the A476T substitution may act as a risk factor for PD upon aging and therefore included it together with the two Spanish PD-associated variants in our functional studies.

Clinical phenotype of A476T variant

The mean age of disease onset in carriers of the A476T variant was 53 years (SD ± 11.7). All patients presented with typical dopa-responsive Parkinsonism and displayed no family history leading to the diagnosis of idiopathic PD. The most frequent genetic cause of sporadic PD in Caucasians, the G2019S mutation in the *LRRK2* gene, was excluded in all symptomatic carriers of the A476T variant in the *mortalin* gene (35). One patient, whose full medical records were available, showed first symptoms at the age of 61 with general slowing of movements, shuffling of gait, intermittent tremor of both upper limbs and reduced olfactory sense. Magnetic resonance imaging revealed slight microcalcifications in the basal ganglia as occasionally observed in asymptomatic persons; however, there is no evidence for a symptomatic Parkinsonian syndrome, i.e. due to vascular lesions. The diagnosis of PD was made by a neurologist experienced in movement disorders. The symptoms responded well to dopaminergic therapy. At the age of 63, the patient reported worsening of motor symptoms with additional difficulties in concentration and dysarthria so that dopaminergic treatment was increased up to a levodopa-equivalent dose of 850 mg/day. No levodopa-related complications were reported, specifically no levodopa-induced psychosis occurred. Neuropsychological testing revealed a cognitive decline beginning at the age of 63. The patient was first tested at this age, when he reported a decline in cognitive capacity. A follow-up test at the age of 66 confirmed mild cognitive deficits without progression over time. Seven years after the diagnosis of PD at the age of 66, the patient unexpectedly died of cardiac failure following an acute myocardial ischemia.

The mother of this patient suffered from a stroke at the age of 85 and died about 10 years later due to cardiac insufficiency. The father suffered from cardiac asthma and died at an early age.

The A476T variant was also identified in one child of the index patient aged 49 years that was clinically unaffected at the time of the neurological examination. Furthermore, we excluded the variant in another child of this patient that displayed no signs of motor impairment at an examination at the age of 51 (Supplementary Material, Fig. S1B and C).

Wt mortalin and mortalin variants in HEK293 and SH-SY5Y cells display intact mitochondrial targeting

Mortalin is a nuclear encoded mitochondrial protein that requires posttranslational transport across the mitochondrial membranes to reach the mitochondrial matrix. To confirm the ability of all mortalin variants to be imported to mitochondria, we studied their subcellular localization by immunocytochemistry in

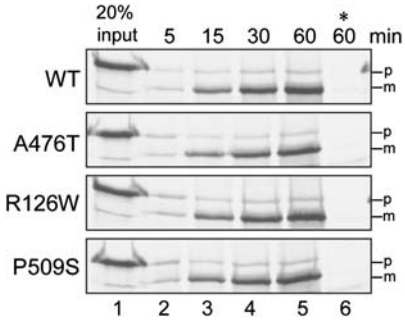

Figure 3. *In vitro* import of wt mortalin and its variants into mitochondria. Radiolabeled precursors of mortalin or its variants were incubated for the indicated time with mitochondria isolated from HeLa cells. Reaction mixtures were incubated at 30°C in the absence (lanes 2–5) or presence (lane 6; asterisk) of CCCP. At the end of the import reactions, proteinase K was added and mitochondria were reisolated by centrifugation before their analysis by SDS–PAGE and autoradiography. The precursor and mature forms of the protein are labeled as p and m, respectively.

HEK293 cells as well as in SH-SY5Y cells transiently transfected with wt mortalin or one of the variants. Using immunocytochemical techniques, we found mitochondrial localization of the recombinant protein for wt mortalin and all three variants in HEK293 cells (Supplementary Material, Fig. S3) and in SH-SY5Y cells (Supplementary Material, Fig. S4). These results cannot exclude the possibility that mortalin variants are only associated on the surface of mitochondria rather than being inside the mitochondrial matrix. To test the import capacity of the variants in more detail, we performed an *in vitro* import assay employing radiolabeled mortalin variants and mitochondria isolated from HeLa cells. The results demonstrate that both, the final efficiency and the kinetic of the import of the variant proteins, are not altered compared with that of wt mortalin (Fig. 3, lanes 2–5). As expected, in the presence of the respiratory chain uncoupler, carbonyl cyanide *m*-chlorophenylhydrazone (CCCP), which acts as a mitochondrial stressor, neither wt nor variant mortalin proteins were imported into mitochondria (Fig. 3, lane 6, asterisk). Taken together, our results suggest that, as observed previously for wt mortalin (16), the mutated versions are also efficiently imported into mitochondria.

Cells overexpressing mortalin variants or wt mortalin have differential effects on intramitochondrial ROS levels

Dysfunction of mitochondria is reflected by impaired oxidative phosphorylation, which leads to the generation of ROS. Mortalin as a mitochondrial chaperone can protect the organelle against such ROS production. Therefore, we monitored ROS levels in dopaminergic SH-SY5Y cells stably overexpressing wt, A476T, R126W or P509S mortalin and in cells transfected with an empty vector as a control. The intramitochondrial ROS production was quantified by flow cytometry using MitoSOX Red, a fluorogenic dye that is targeted to the mitochondria and is readily oxidized by superoxide species. ROS production was monitored under basal conditions and under the induction proteolytic stress (Fig. 4A). Under basal conditions, analysis of MitoSOX Red fluorescence demonstrated significantly lower amounts of ROS in

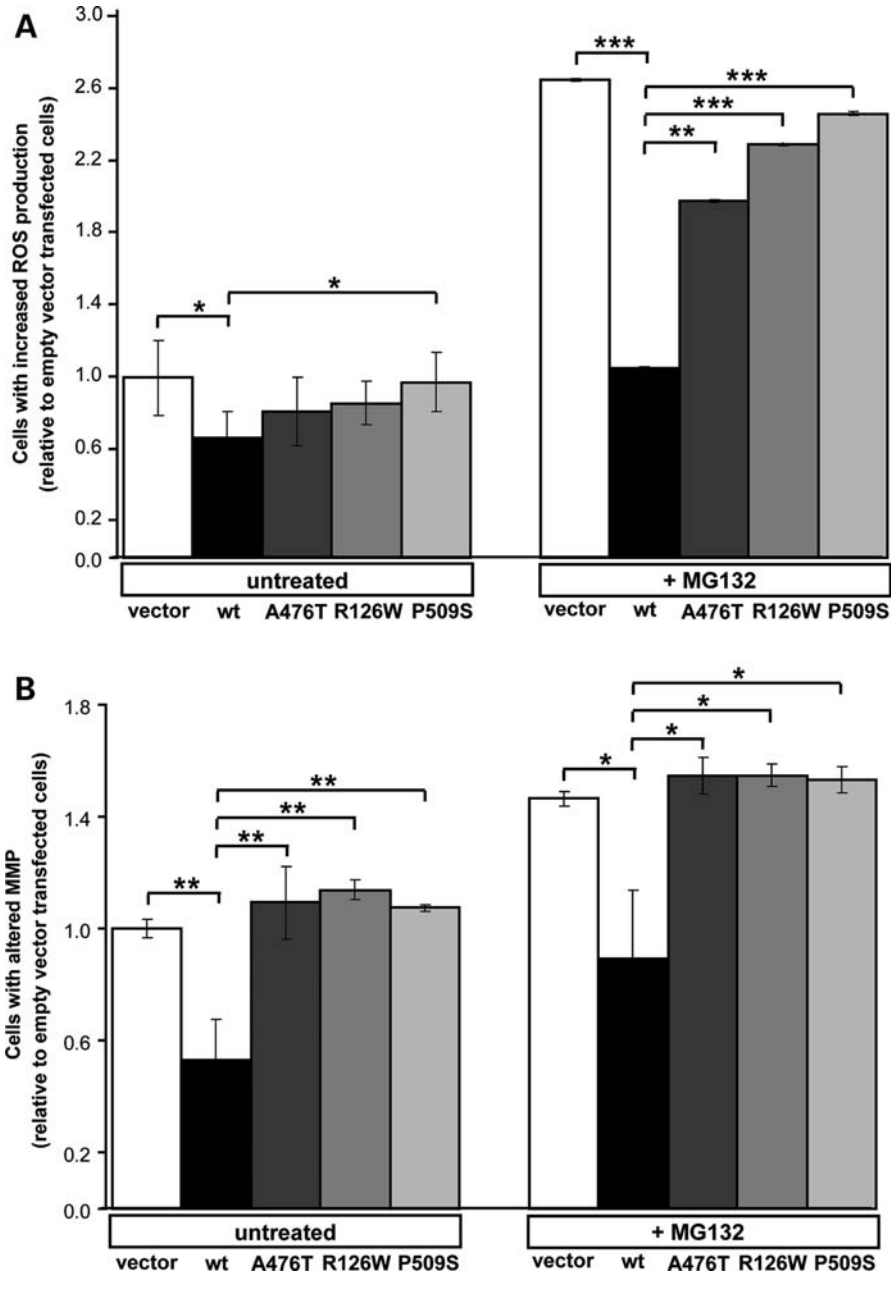

Figure 4. Effects of mortalin on mitochondrial homeostasis under basal conditions and under the induction of proteasomal stress in SH-SY5Y cells. (**A**) Measurement of MitoSOX Red fluorescence signal of untreated SH-SY5Y cells and paradigm with the treatment of the proteasome stressor MG-132. The results were normalized to the empty vector control. An increased fluorescence signal correlates with a higher amount of ROS. The left panel shows ROS levels under basal conditions. Overexpression of wt mortalin indicates a significantly lower production of ROS compared with the overexpression of P509S mortalin or vector control ($P < 0.05$). The right panel shows ROS levels under conditions of proteasomal stress induced by MG-132. Compared with cells overexpressing one of the mortalin variants or the vector control, cells overexpressing wt mortalin exhibited significantly reduced ROS levels ($P < 0.01$ for A476T mortalin; $P < 0.001$ for R126W mortalin, P509S mortalin and control). All experiments were performed in duplicate and repeated at least three times. Data are presented as means ± SD. (**B**) Measurement of TMRE fluorescence signal of untreated as well as MG-132-treated SH-SY5Y cells to monitor the MMP by flow cytometry. Analysis of TMRE fluorescence demonstrated an improved MMP in cells overexpressing wt mortalin compared with cells expressing one of the mortalin variants or the vector control ($P < 0.01$; left panel). After treatment with the proteasomal inhibitor MG-132, cells overexpressing one of the variants or the vector control demonstrated significant alterations of MMP compared with cells overexpressing wt mortalin ($P < 0.05$; right panel). Data are indicated as mean ± SD of three independent experiments.

cells overexpressing wt mortalin compared with control cells ($P < 0.05$; Fig. 4A, left panel). This reduction of ROS was less pronounced for all mortalin variants, with significantly different levels observed for P509S mortalin-overexpressing cells compared with wt mortalin-overexpressing cells.

Next, we examined whether the application of the proteasomal inhibitor MG-132 to SH-SY5Y cells stably overexpressing wt mortalin or mortalin variants might modulate the intramitochondrial ROS production. When cells were subjected to proteolytic stress induced by MG-132 (Fig. 4A, right panel),

both, cells overexpressing one of the variants of mortalin and control cells, showed a significantly increased MitoSOX Red fluorescence after treatment compared with cells overexpressing wt mortalin ($P < 0.01$ for A476T mortalin; $P < 0.001$ for R126W mortalin, P509S mortalin and control). Of note, the different variants of mortalin do not protect SH-SY5Y cells from proteolytic stress as efficiently as the wt protein.

Cells overexpressing mortalin variants or wt mortalin have differential effects on mitochondrial membrane potential

Next, we examined changes in mitochondrial membrane potential (MMP) as a further marker of impaired mitochondrial function. MMP was examined by flow cytometry in SH-SY5Y cells stably overexpressing wt mortalin and its variants. Using tetramethylrhodamine ethyl ester perchlorate (TMRE) fluorescence to monitor the MMP, we were able to find significant differences in cells with altered MMP under basal conditions. In comparison with empty vector control, cells overexpressing wt mortalin showed a significantly improved MMP ($P < 0.01$) (Fig. 4B, left panel). This change in the MMP was not observed for the mortalin variants showing similar MMP levels like the empty vector control.

Next, we examined whether proteolytic stress affects the MMP of the various cells (Fig. 4B, right panel). As seen above, treatment of cells with MG-132 resulted in a significant alteration of the MMP. These changes in the MMP were significantly less pronounced for cells overexpressing wt mortalin compared with empty vector control or cells overexpressing one of the mortalin variants ($P < 0.05$).

Cells overexpressing mortalin variants or wt mortalin have differential effects on mitochondrial morphology

Recent studies indicate that dynamic morphological alterations of mitochondria are related to mitochondrial dysfunction (36). Therefore, we applied live-cell-imaging technique based on SH-SY5Y cells cotransfected with Mito-DsRed plasmid and wt mortalin or one of the variants (ratio 1:4). We found significant differences in the mitochondrial morphology between cells overexpressing wt mortalin and cells overexpressing one of the disease-associated variants or the empty vector (Fig. 5A and B). Semi-automated analysis of mitochondrial morphology, which includes parameters such as the length (aspect ratio—AR) and degree of branching (form factor—FF) from single cells ($n = 222$), revealed increased branching of mitochondria in cells overexpressing wt mortalin compared with cells overexpressing any of the mortalin variants. wt mortalin-overexpressing cells display a significant increase in connectivity ($P < 0.001$) and elongation ($P < 0.05$) compared with the empty vector control. This effect of mortalin was significantly less pronounced in cells overexpressing R126W and P509S mutant mortalin in terms of connectivity (FF; $P < 0.001$) and elongation (AR; $P < 0.001$). SH-SY5Y cells overexpressing A476T mortalin revealed a less interconnected mitochondrial network than wt mortalin-overexpressing cells (FF; $P < 0.001$); however, no significant alterations of mitochondrial length were observed (AR). These results show that in contrast to cells overexpressing wt mortalin, the overexpression of A476T, R126W or P509S mortalin in SH-SY5Y cells is significantly less potent in changing mitochondrial morphology.

As mitochondrial morphology is regulated by key proteins that control mitochondrial fission [dynamin-related protein 1 (Drp1) and hFis1] or fusion [mitofusin 2 (Mfn2) or OPA1] events, we next assessed the potential influence of mortalin on these fusion–fission regulators. Using western blot (WB) analysis to detect a potential effect of mortalin on the steady-state levels of the fission factors Drp1 and hFis1 or the fusion factors OPA1 and Mfn2, we observed neither an increase in fission-mediating proteins, nor a decrease in fusion factors as a cause of the observed mitochondrial phenotype (data not shown).

Wt mortalin but not mortalin variants rescues functional impairments in knockdown models

To assess the effect of loss of mitochondrial mortalin on mitochondrial function, we measured MMP and ROS production by fluorescent-activated cell sorting (FACS) analysis in HEK293 cells depleted partially of their endogenous mortalin by an siRNA-mediated process. Mortalin protein was efficiently downregulated as demonstrated by immunoblotting (Fig. 6A). Densitometric analysis revealed a knockdown efficiency of endogenous mortalin protein of >50% compared with the status of cells treated with control siRNA (Fig. 6B). The levels of mortalin in these cells could be restored to >80% of the expression level in control cells.

We first tested whether siRNA-mediated knockdown of endogenous mortalin modifies the levels of ROS production and whether transfection of wt mortalin or disease-associated variants would restore the phenotype. For this, we utilized the FACS technique using MitoSOX staining. Knockdown of endogenous mortalin caused a significant increase of intramitochondrial ROS production compared with control siRNA-treated cells ($P < 0.01$; Fig. 7A). We then investigated whether these functional abnormalities induced by mortalin knockdown could be restored by reintroduction of plasmid-encoding wt mortalin or one of the disease-associated variants. Reintroduction of wt mortalin, but not R126W mortalin or P509S mortalin, restored intramitochondrial ROS levels ($P < 0.05$). Cells transfected with A476T mortalin showed a similar tendency; however, the statistic significance of the results was low ($P = 0.056$).

Next, we measured the effect of mortalin knockdown on MMP by TMRE staining. FACS analysis revealed that transfection with *mortalin* siRNA resulted in a reduction of intact MMP in 25% of the HEK293 cells compared with cells transfected with non-targeting control siRNA ($P < 0.05$; Fig. 7B). The impaired MMP after mortalin knockdown could be rescued by wt mortalin, but not by the R126W or P509S mortalin variants ($P < 0.01$). Again, cells transfected with A476T mortalin showed a similar tendency; however, the changes in MMP were not significant ($P = 0.069$). These observations are consistent with a loss of the physiological function in mortalin variants.

Human fibroblasts from the carrier of the A476T variant display changes in mitochondrial morphology

Finally, we extended our morphological studies of mitochondria to human fibroblasts. The mitochondrial morphology of

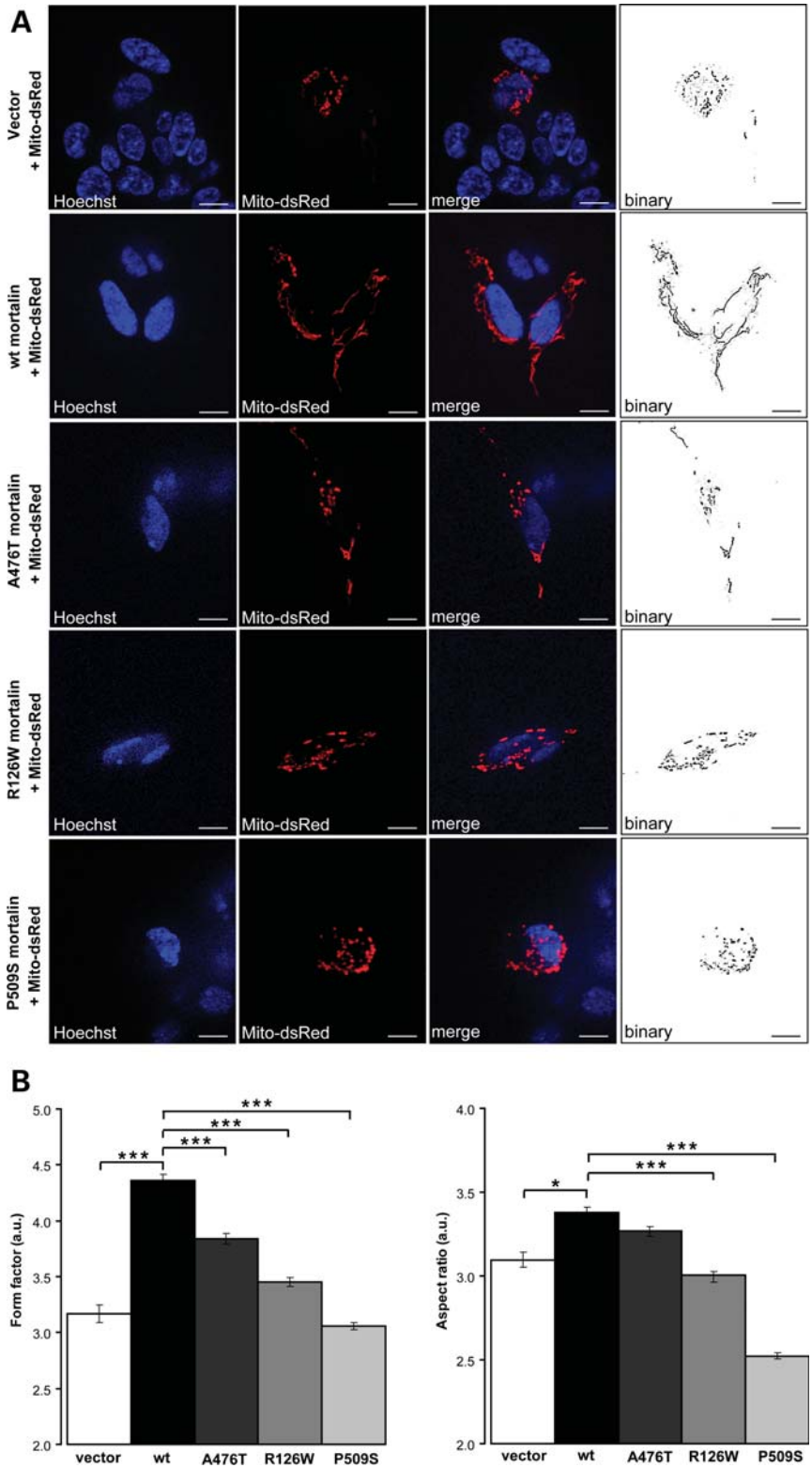

Figure 5. Effect of mortalin on mitochondrial morphology in SH-SY5Y cells. (**A**) Mitochondrial morphology in living SH-SY5Y cells transiently cotransfected with Mito-DsRed (red) and wt mortalin, its disease-associated variants or the empty vector in the ratio 1:4 was analyzed by live-cell-imaging microscopy (Cell Observer Z1, Zeiss) at 37°C using ApoTome® optical slides with 0.240–0.300 μm *z*-stacks. Forty-eight hours after cotransfection, nuclei were stained with Hoechst 33342 (blue). The respective stainings were merged and mitochondria were analyzed using Image J 1.41o software for area, perimeter, major and minor axes based on binary images, which only have two possible values (black/white) for each pixel. On the basis of these parameters, the AR of a single mitochondrion and its FF were calculated. (**B**) Mitochondrial branching as indicated by the FF was significantly increased in SH-SY5Y cells cotransfected with Mito-DsRed and wt mortalin compared with cotransfection with empty vector or one of the mortalin variants ($P < 0.001$; left panel). Mitochondrial length as indicated by the AR was significantly increased in cells overexpressing wt mortalin compared with R126W mortalin or P509S mortalin ($P < 0.001$) as well as in cells transfected with the empty vector ($P < 0.05$; right panel). Images from 222 individual cells were analyzed from three independent experiments. Data are presented as mean ± SE of three independent experiments.

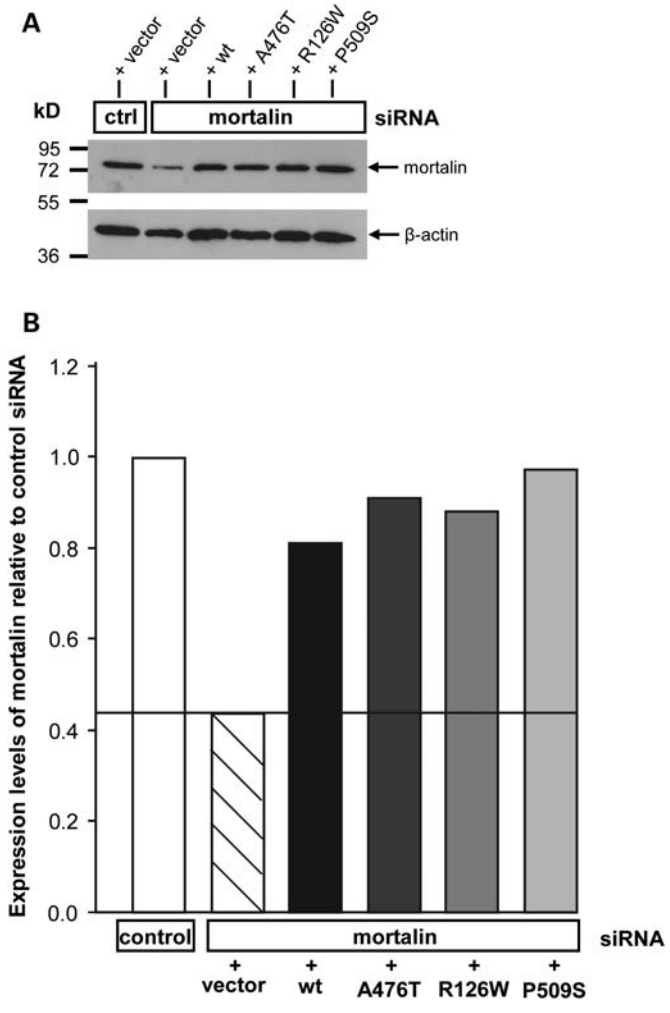

Figure 6. Expression levels of mortalin in a knockdown model. (**A**) WB analysis of the *mortalin* siRNA-mediated knockdown effect on endogenous mortalin (lane 2) as well as retransfection levels of recombinant wt (lane 3), A476T (lane 4), R126W (lane 5) and P509S (lane 6) mortalin following siRNA treatment. The effect of the addition of *mortalin* siRNA *per se* was controlled by the use of an unmodified non-targeting control siRNA (lane 1). We used an antibody against mortalin to control for expression levels of endogenous mortalin, and anti-β-actin was used as loading control. (**B**) Densitometric analysis of the WB shown in (A). In respect to cells treated with control siRNA (lane 1), downregulation of mortalin by use of siRNA and retransfection of the empty vector resulted in 57% of control levels (lane 2). The rescue effect observed by retransfection of wt mortalin (lane 3) or one of the mortalin variants (lanes 4–6) was between 81 and 97% compared with cells treated with control siRNA.

fibroblasts from a heterozygous carrier of the A476T variant and from a sibling control carrying the homozygous wt allele was monitored (Fig. 8A). We found that control fibroblasts exhibited large interconnected mitochondria, whereas fibroblasts from the carrier of the A476T variant were significantly shorter and fragmented (FF; $P < 0.001$ and AR; $P < 0.001$; Fig. 8B). Therefore, our analysis of human fibroblasts ($n = 82$) from the heterozygous carrier revealed a mitochondrial phenotype with a reduced tubular network. These findings underscore a role for mortalin in the regulation of mitochondrial morphology, similar to our observation in SH-SY5Y cells overexpressing mortalin variants (Fig. 5).

DISCUSSION

Aging as a major risk factor for PD shares typical biochemical alterations with neurodegenerative processes due to impaired mitochondrial function, i.e. increased levels of oxidative damage and impaired cellular energy supply. Indeed, the role of unbalanced mitochondrial homeostasis in PD has been recently supported by the identification of variants in nuclear encoded proteins that are responsible for mitochondrial dysfunction and impaired dynamics, i.e. Parkin (PARK2), PINK1 (PARK6), DJ-1 (PARK7) and Omi/HtrA2 (PARK13) (4,37–40). The mitochondrial chaperone protein mortalin has been linked to PD pathogenesis based on reduced levels in affected brain regions of sporadic PD patients and its interaction with the PD-associated protein DJ-1 (12,30). Here, we confirm this interaction and provide first functional evidence for a direct contribution of aberrant mortalin to impaired mitochondrial function and dynamics in PD.

Using an unbiased proteomic approach to screen for DJ-1-interacting proteins, we confirmed previous reports of the interaction of DJ-1 with mortalin using independent proteomic techniques (12,13). Therefore, we hypothesized that mortalin may also act in signaling pathways responsible for mitochondrial stress response and the maintenance of mitochondrial integrity similar to that of the redox-sensing protein DJ-1 (8).

All currently identified disease-associated variants of the *mortalin* gene were observed in the heterozygous state. Although heterozygosity of these variants in the *mortalin* gene suggests an autosomal dominant effect, due to the lack of a reported family history in the respective patients, it is more likely a genetic trait with reduced penetrance and argues in favor of a genetic susceptibility factor for PD. Since the complete loss of mortalin function is not compatible with cell survival as observed in different models from yeast to vertebrates (41), heterozygous variants in the *mortalin* gene would be in line with the concept of a risk factor contributing to a late onset of neurodegenerative disease. Indeed, genetic studies for susceptibility factors in the common late onset form of PD showed that the sporadic appearance of the disease does not preclude an involvement of genetic factors in the pathogenesis of PD (42). Further support for a potential role of mortalin in PD pathogenesis is derived from a substantial number of genomic screens that have consistently shown a susceptibility locus for PD on the long arm of chromosome 5, which harbors the *mortalin* gene located at 5q31.1 (42–45).

First evidence for the pathogenic relevance of the novel variants in the mortalin protein came from interspecies comparisons of the mortalin amino acid sequence that showed complete conservation of the respective amino acid residues from vertebrates to yeast (Fig. 2B–D). The functional domains of the mortalin protein include the ATPase domain and the substrate-binding domain (46). The A476T and the P509S variants are located in the substrate-binding domain, whereas the R126W variant affects the ATPase domain of the protein. Irrespective of their localization, our results argue in favor of a loss of protective mortalin function in the mitochondria. In fact, we found that cells overexpressing one of the mortalin variants were more susceptible to increased mitochondrial oxidative stress compared with wt

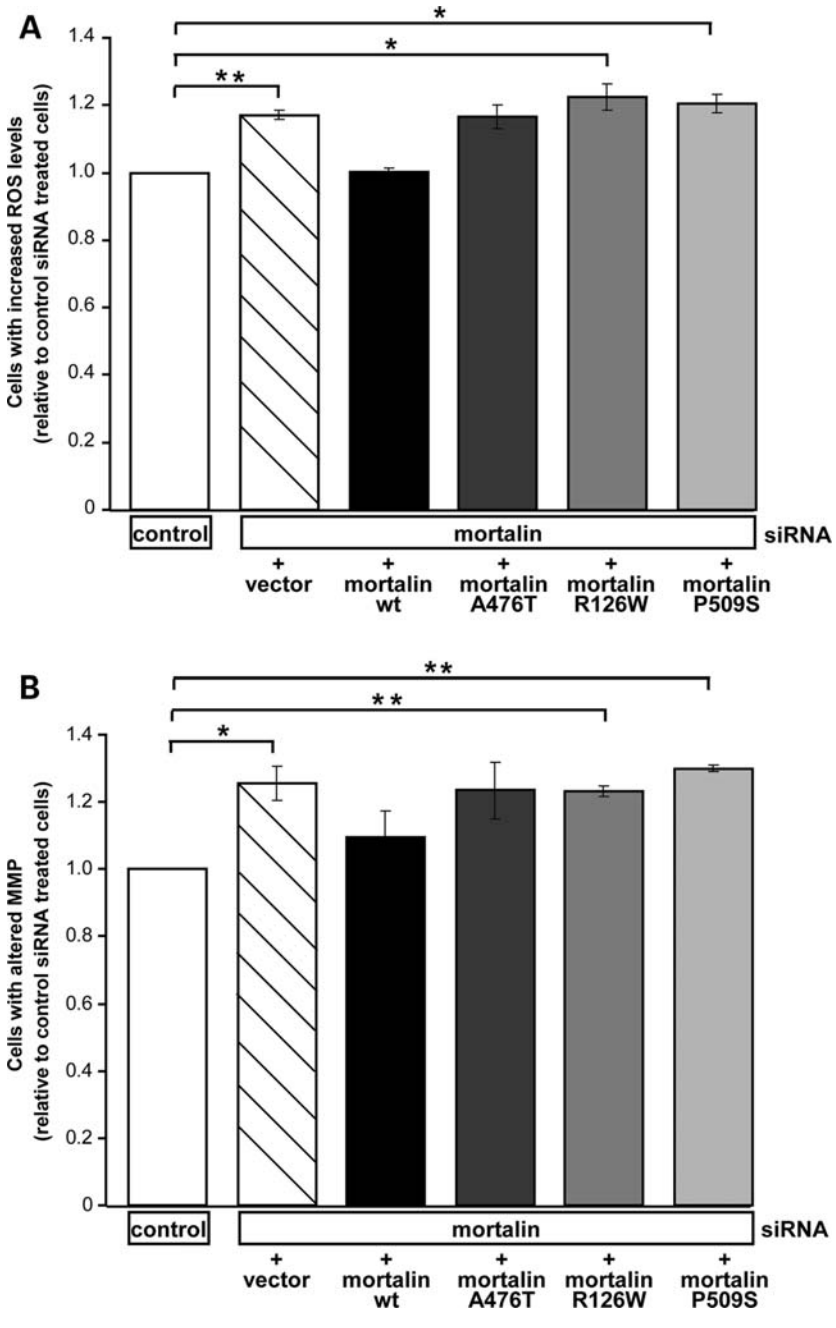

Figure 7. Effect of downregulation of mortalin on mitochondrial function. (**A**) ROS production as indicated by the level of MitoSOX Red fluorescence signal was significantly increased in *mortalin* siRNA-transfected HEK293 cells relative to control siRNA-transfected cells ($P < 0.01$). Transfection of siRNA-treated cells with wt mortalin showed a complete rescue of this mitochondrial phenotype. Rescue with A476T mortalin was partially achieved, whereas transfection with R126W or P509S mortalin variants failed to restore this mitochondrial phenotype ($P < 0.05$ compared with control siRNA-treated cells). (**B**) Measurement of TMRE red fluorescence signal revealed a significant increase of altered MMP in HEK293 cells transfected with *mortalin* siRNA compared with control ($P < 0.05$). Restoration of this signal could be observed by transfection of wt mortalin, but not with R126W or P509S mortalin variants. Partial rescue was observed by transfection of A476T mortalin. Data are indicated as mean ± SD of three independent experiments.

mortalin-overexpressing cells. Furthermore, using a knockdown model of mortalin in human cells, we found that the reported variants were unable to restore the observed mitochondrial phenotype, thus confirming the loss-of-function hypothesis. Indeed, the observed ~50% knockdown of wt mortalin in these cells is compatible with a model of haploinsufficiency for mortalin function. This model is also in line with the mitochondrial phenotype, which we observed in fibroblasts from the heterozygous carrier of the A476T variant and is characterized by a reduced mitochondrial connectivity.

We have confirmed the mitochondrial localization of wt mortalin by an *in vitro* import assay and immunocytochemistry. All disease-associated mortalin variants showed the same *in vitro* import kinetics and these results are supported by our immunocytochemical studies in human cells. Thus, the various mutations in the variants do not affect the

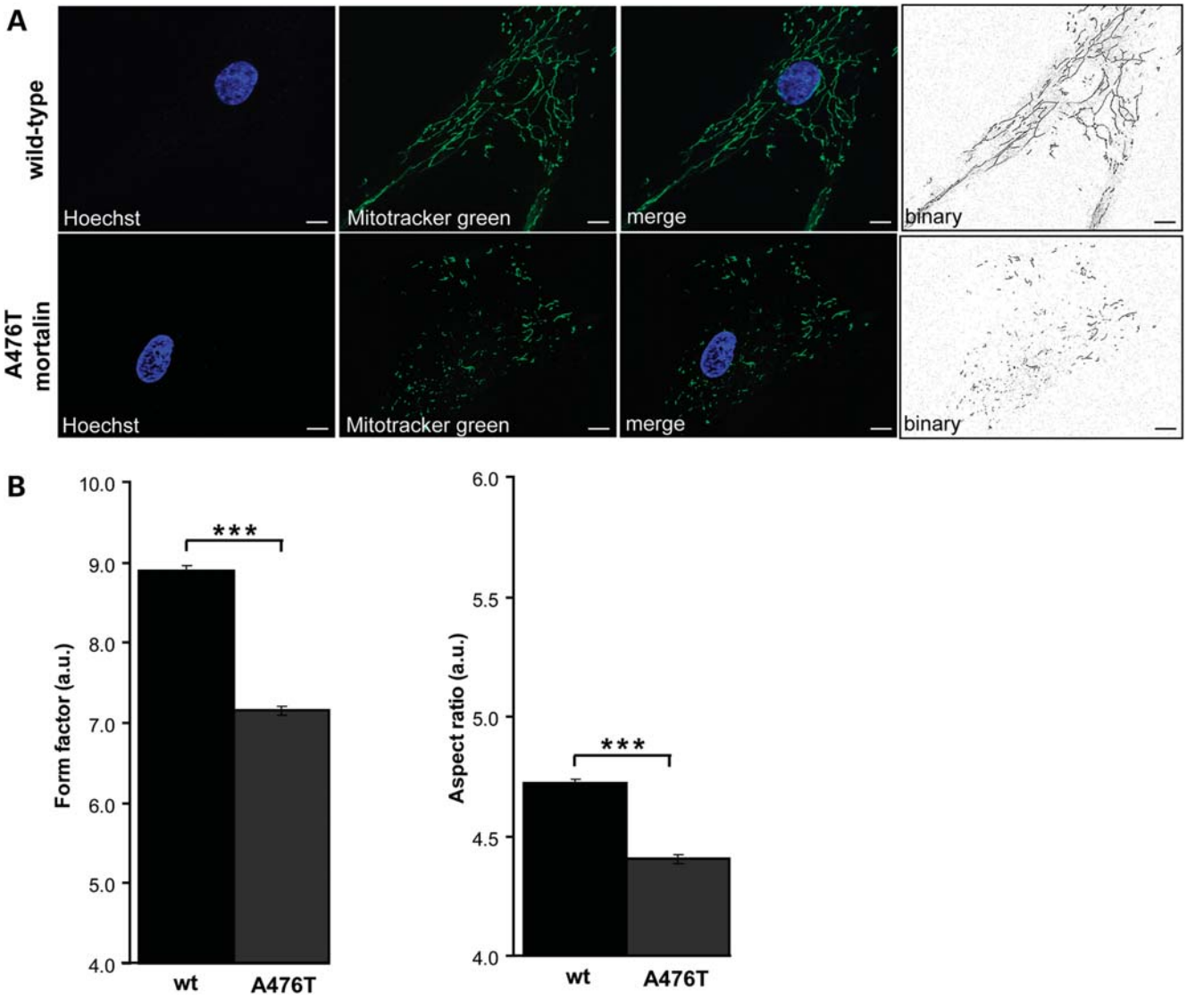

Figure 8. Effect of mortalin on mitochondrial morphology in human fibroblasts. (**A**) Mitochondrial morphology in living human fibroblasts from a carrier of the A476T variant and a healthy sibling control were analyzed by live-cell-imaging microscopy at 37°C using ApoTome® optical slides with 0.240–0.300 *z*-stacks. Mitochondria were stained with 200 nM of the specific mitochondrial dye MitoTracker® green FM (green) for 15 min at 37°C; nuclei were stained with Hoechst 33342 (blue). The respective stainings were merged and mitochondria were analyzed using Image J 1.41o software for area, perimeter, major and minor axes based on binary images. The calculation of the AR and FF was done as described in Figure 5. (**B**) Mitochondrial branching as indicated by the FF was significantly reduced in fibroblasts from the carrier of the A476T variant in comparison with control fibroblasts ($P < 0.001$) (left panel). Mitochondrial length as indicated by the AR was significantly reduced in fibroblasts from the carrier of the A476T variant in comparison with control cells (right panel). Eighty-two individual cells were analyzed from three independent experiments. Data are indicated as mean ± SE of three independent experiments.

subcellular localization of the protein, indicating that the observed differences in the levels of ROS and MMP compared with wt mortalin were not due to defective import of the mortalin variants into mitochondria, but rather due to a loss-of-functional mortalin within the mitochondrial matrix.

Indeed, due to their high metabolic activity, mitochondria are notably exposed to ROS and are at risk of oxidative damage to their DNA, lipids or proteins. Specifically for dopaminergic neurons that are reported to have a constitutively lower mitochondrial mass (47), the integrity of a functional protein clearance machinery is critical for mitochondrial function. In mitochondria, effective refolding of damaged proteins by chaperones or targeting for proteolytic cleavage is mediated by specific proteins, of which Omi/HtrA2 has been recently identified as an important part of the mitochondrial protein quality control (48). Mortalin was reported to be involved in protein refolding in the mitochondrial matrix compartment due to coupling with the mitochondrial Hsp60 protein (49). Moreover, the yeast homologue of mortalin is known to target misfolded proteins to mitochondrial proteases for degradation (50). Indeed, we found that overexpression of wt mortalin is protective in paradigms of proteolytic stress as assessed by intramitochondrial ROS and maintenance of the MMP. In contrast, the disease-related mortalin variants were devoid of this protective function and did not differ from controls.

Therefore, we speculate that misfolding of mortalin and/or impaired interaction with intramitochondrial substrates and interaction partners might interfere with the protective role of mortalin in maintaining mitochondrial function. Indeed, increased proteolytic stress has been shown to predispose to misfolding of mortalin, resulting in defective protein import into mitochondria and mitochondrial morphology in yeast (51). More interestingly, the loss of function of Ssc1p, the yeast homologue of mortalin, resulted in the disintegration of the mitochondrial network and the formation of aggregates. This was not due to impairments of mitochondrial import, but rather due to the effects of the yeast mortalin homologue within the matrix (52). These results support our findings and reveal a similar morphological phenotype of loss of mortalin function in yeast and human cells. Therefore, our results underscore the crucial involvement of mortalin in the maintenance of mitochondrial morphology due to its function in the mitochondrial matrix.

Several proteome-based studies from postmortem brains of PD patients and controls revealed reduced levels of mortalin in affected brain regions (22,30,53). In addition, the amount of mortalin not only turned out to be a marker for sites of neurodegeneration in PD, but also a correlation of protein levels with disease progression was reported with a further decrease of mortalin in advanced stages of PD (53). Together with the loss of function variants in the *mortalin* gene described here in PD patients, the critical role of functional mortalin in neurodegeneration in PD becomes evident. Therefore, large genetic studies in different populations of PD patients and subsequent functional studies are required to further dissect the contribution of sequence variations in the *mortalin* gene to the pathogenesis of PD.

MATERIALS AND METHODS

Patients and controls

A detailed mutation analysis of the *mortalin* gene in a large sample of 286 German sporadic and familial PD patients was performed after obtaining informed consent. All patients were evaluated by a neurologist and were diagnosed as idiopathic PD, based on the UK Parkinson's Disease Brain Bank criteria (54). The mean age of disease onset was 57.2 years ($\pm$ 11.3). Ethical approval was obtained by the Ethics Committee of the University of Tübingen. A total of 290 healthy German individuals closely matched for age and gender served as controls after a standardized neurologic examination to exclude participants with clinical signs of PD or any other extrapyramidal disorder (mean age: 72 $\pm$ 4.3 years; males: 52%, females: 48%).

The three mortalin variants A476T, R126W and P509S were subsequently genotyped in an independent cohort consisting of 1008 German sporadic PD patients and 1342 German population-based controls. The PD cases were collected by movement disorder specialists of the Universities of Munich and Tübingen, who established the diagnosis according to the UK Brain Bank criteria. The mean age at onset was 56.0 $\pm$ 12.1 years. All subjects gave written informed consent and the study including DNA collection was approved by the local ethics committees. The control individuals were selected from the KORA survey (Cooperative Health Research in the Region of Augsburg, www.helmholtz-muenchen.de/kora), a population-based study. The samples were genotyped using the matrix-assisted laser desorption/ionization time-of-flight mass spectrometry method (MassArray system, Sequenom).

PCR conditions and restriction length polymorphism analysis

Based on the published genomic sequence of the human *mortalin* gene on chromosome 5q31.1 (NCBI accession number NM_004134), we performed a detailed mutational screening of the coding sequence that includes 17 exons and adjacent intronic regions. Primers to amplify the respective sequences of the *mortalin* gene were generated using the online software Primer3 (http://frodo.wi.mit.edu/primer3/input.htm; Table 2). PCR reactions were carried out in a Thermocycler PTC Dyad 220 (MJ Research, Biozym, Germany) using the following conditions: 100–500 ng DNA were amplified in a final volume of 26 μl in the presence of PCR Buffer (Promega, USA), 200 μM of each dNTP, 10 pmol of each PCR primer and 0.5 units of Taq Polymerase (Promega). Standard cycling conditions were established using a touchdown protocol: 5 min at 94°C; 10 times: 30 s at 94°C, 30 s at 65°C (−1°C per cycle), 30 s at 72°C; 30–35 times: 30 s at 94°C, 30 s at 55°C, 30 s at 72°C; followed by a final elongation for 6 min at 72°C.

For the subsequent genotyping of the c.1426G>A variant in exon 12 of the *mortalin* gene, the entire PCR product was digested by adding 15 units of the restriction enzyme *Sat*I (MBI Fermentas, USA) to the reaction mixture in a final volume of 45 μl. Restriction fragments were visualized on a 2% agarose gel stained with ethidium bromide.

dHPLC analysis and sequencing

Prepared DNA samples from PCR were screened for variants using dHPLC analysis on the WAVE™ DNA Fragment Analysis System (Transgenomic, USA). For the mutational screening, the resulting PCR products from two patients were pooled at a 1:1 ratio followed by a denaturation step at 94°C and subsequent renaturation over 15 min by cooling down the sample to 10°C gradually. This allows the formation of heteroduplexes even in the presence of homozygous sequence variations. Column temperatures and running conditions were established using Wavemaker™ Software (Version 4.1.31, Transgenomic) and are given in Table 2. DNA samples exhibiting curve patterns suspicious for heteroduplexes were sequenced on an ABI Prism® Sequence Detecting System (3100 Genetic Analyzer) using the ABI BigDye® Terminator v3.1 Cycle Sequencing Kit (Applied Biosystems, USA) with primers used for exon amplification.

GST pull-down assay and mass spectrometry

Screening for novel interacting proteins of DJ-1 was performed by a GST pull-down assay. Recombinant GST-DJ-1 protein was produced by cultivation of *Escherichia coli* cells transformed with pGEX-6P-3-DJ-1. Cells were collected by

Table 2. Analysis of the coding exons of the *mortalin* gene: PCR and dHPLC conditions and identified nucleotide and amino acid substitutions

Exon	Primer, forward	Primer, reverse	Product length (bp)	Annealing temperature (°C)	Column temperature (dHPLC) (°C)	Nucleotide substitution	Amino acid substitution
1	5′-TGG TTG GAG GTT TCC AGA AG-3′	5′-AAT TCA AAC CCT AAA GGG CG-3′	275	a	63.5; 66.6	c.−31T>C; c.81+6G>A	*n*
2	5′-TTC TCT TTT TCC TCC CAG GAT-3′	5′-TTC CCT CTC AAA GGA AAT GA-3′	152	a	56.0; 58.0	*n*	*n*
3	5′-TCC AGT GAC TTT GGT CTA TCA AGA-3′	5′-AAA GCG CAA ATC AGG TTC TC-3′	246	60	55.2; 57.4	*n*	*n*
4	5′-CTC TCT ATC ACA TTT TGG GAG TTT-3′	5′-CAT GCT GAG GCT CTT CTG TG-3′	278	a	58.2; 61.4	c.243C>T	Ala81Ala
5	5′-TGG TAT GTG GTA ATT TTG TCA TGG-3′	5′-CTA GTG ATC TCA CAG GAA TCA TTG-3′	259	a	54.6; 58.0	*n*	*n*
6–7	5′-GCT GCA AAA GGA TGA CAC AG-3′	5′-CAG TAA AAG CAC TGT AAA AGG CTC-3′	447	a	55.0; 57.3	*n*	*n*
8	5′-ATC CTG GTG ATA GGT TTT GTT C-3′	5′-AAG AGT ATC TGT GTC TAG AAT AAG GGG-3′	348	a	54.6; 58.0	c.774G>A; c.879+80C>T; c.717-27_717-26insT; c.872_879+9dup17	Gln258Gln
9	5′-TGT GTT GTT CCA CCT TAT TAC TGC-3′	5′-TTT TAA ATA AGC TCC GGC TG-3′	235	a	57.3; 59.2	c.948A>G; c.880−49_52delTTTA oder c.880 − 53_56delTTTA	Lys316Lys
10	5′-AAA TGT AAC CGT CAT TTG GC-3′	5′-GGC CAT ATA TTT GTG CCA CC-3′	350	55	57.8	*n*	*n*
11	5′-ACA CGT GCT CCC TTT TGT TC-3′	5′-GGC TGC AAT TAC ATC CGT C-3′	368	a	56.5; 60.0	*n*	*n*
12	5′-TCT TGG AAT GTA AAC CTT TGG C-3′	5′-CAG TAT GTA TGT GTA TGC CAG CAG-3′	305	a	55.7; 57.7	c.1426G>A; c.1411 − 16G>T	Ala476Thr
13	5′-AAT AGC ACT GGA CCC CTC TG-3′	5′-GGG TCT ATT CCC AAG ACC TCC-3′	234	a	55.8; 57.8	*n*	*n*
14	5′-TGC AAT GGA GGA AGA AGA GG-3′	5′-CCC AAA CTC CCA CTG TCA AG-3′	229	a	55.9	*n*	*n*
15	5′-TGG TTG ATT GGA AAG TCT TCG-3′	5′-CCC CTA TCA AAA CCC ACA GA-3′	225	a	56.2	*n*	*n*
16	5′-TGG TAC AGG AGA CCT GGA AAA-3′	5′-AAA ATC CAC TTC AGC CCT TG-3′	213	a	56.0; 58.4	c.1933C>T	Leu645Leu
17	5′-AAC GTT AAA TCT GAG TGG CTC T-3′	5′-TGT TGT CCT TCT GGC TTC AA-3′	166	a	56.5; 58.5	*n*	*n*

[a]Touch-down protocol: 94°C → 5′; [94°C → 30″, 65°C →30″ (−1°C per cycle), 72°C → 30″] 10×; (94°C → 30″, 55°C →30″; 72°C → 30″) 30×; 72°C → 6′; 8°C → ∞.

centrifugation and the pellet was resuspended using lysozyme and protease inhibitor cocktail Complete® (Roche, Germany). After complete ultrasonic lysis of the bacteria (cycle continued, output 70%, Bandelin Sonoplus GM70, Gandelin, Germany) and centrifugation, the supernatant contained the fusion proteins that were then bound to glutathione agarose (Molecular Probes, USA). After washing, the recombinant DJ-1 proteins were eluted from the agarose in several steps. Fractions of the elution that contained the recombinant protein were unified and the concentration was determined by a Bradford assay. Then 1 mg of enriched GST-DJ-1 fusion protein was incubated with lysates from SK-N-BE cells, and, as a control, the same cell lysate was incubated with glutathione agarose alone. Samples were run on a sodium dodecyl sulfate–polyacrylamide gel electrophoresis (SDS–PAGE) and stained with Coomassie. Bands of interest underwent tryptic digestion. Resulting peptides were separated via reverse-phase liquid chromatography (Dionex Ultimate, Dionex, Idstein, Germany) coupled online to a mass spectrometer (QStar Pulsar i, Applied Biosystems, Germany) as described previously (55). Mass spectrometry data was processed using OpenMS1.5 (56,57) and Mascot2.2 (MatrixScience, UK) with the following settings: peptide and fragment mass tolerance 0.25, carbamidomethyl as fixed modifications and methionine oxidation as variable modification. An in-house-curated database (IPI_human 3.56; 2009-03-19) containing reverse peptides as well as a list of typical contaminants was used for peptide identification with an expected cut-off score >0.05.

Cloning of wt mortalin and mortalin variants

cDNA of mortalin was obtained from the German Resource Center for Genome Research (RZPD; IRAUp969A034D) and cloned into the *Bam*HI and *Xho*I sites of a pcDNA3.1/V5-His A vector (Clontech, USA) using 5′-TTAGGATCC ATGATAAGTGCCAGCCGAGCT-3′ as a forward primer and 5′-AGCCTCGAGCTGTTTTTCCTCCTTTTGATCTTC-3′ as a reverse primer. The A476T variant was introduced into the wt sequence by the QuikChange® XL Site-directed Mutagenesis Kit (Stratagene, USA). The following primer pairs were used for the insertion of the A476T variant: 5′-AG GTATTCTCTACTGCCACTGATGGTCAAACGCAA-3′ and 5′-TTGCGTTTGACCATCAGTGGCAGTAGAGAATACC T-3′. For the insertion of the R126W variant, primer pairs were used as follows: 5′-CAAGCGTCTCATTGGCTGG CGATATGATGATCC-3′ and 5′-GGATCATCATATCG CCAGCCAATGAGACGCTTG-3′. Lastly, the following primer pairs were used for the insertion of the P509S variant: 5′-GGACAGTTTACTTTGATTGGAATTTCACC AGCCCCTCG-3′ and 5′-CGAGGGGCTGGTGAAATT CCAATCAAAGTAAACTGTCC-3′. All constructs were verified by DNA sequencing.

Transfection, generation of stable cell lines and primary cell culture

SH-SY5Y cells were cultured in a 5% CO_2 humidified atmosphere in Dulbecco's modified Eagle's medium (DMEM) containing 1% penicillin and streptomycin and 15% fetal calf serum (FCS). Transfections were performed using Lipofectamin™ 2000 Reagent (Invitrogen, USA) according to the manufacturer's instructions. To generate polyclonal stable cell lines, 700 000 SH-SY5Y cells were transfected with the pcDNA3.1/V5-His A vector containing wt mortalin or one of its variants (A476T, R126W, P509S) or an empty vector as a control and maintained in medium containing 1 mg/ml G418 (Biochrom, Germany) for selection. Stable expression of wt mortalin and mortalin variants was confirmed by immunoblotting.

Moreover, fibroblasts from offspring of the index patient carrying the A476T variant in the *mortalin* gene were included in our analyses. Skin biopsies were taken from one offspring carrying the heterozygous A476T variant as wells as a sibling control carrying the homozygous wt allele. The carrier of the A476T variant did not show signs of PD at the time of the biopsy. The study was approved by the ethics committee of the University of Tübingen. All patients and controls gave written and informed consent. Primary fibroblast cells were maintained in RPMI medium with 15% FCS supplemented with 100 IU/ml penicillin, 100 mg/ml streptomycin and 1 mM pyruvate. For live-cell-imaging experiments, passage number of fibroblasts <10 were used. Only fibroblasts with the same passage number were taken for analyses.

Western blot

WB analyses were conducted as described previously (4). In the present study, proteins were detected using antibodies against mortalin (anti-GRP75, Santa Cruz Biotechnology, USA), V5 (anti-V5, Chemicon, USA) and β-actin (anti-β-actin, Sigma, Germany). Secondary antibodies were purchased from GE Healthcare (UK) and either diluted 1:10 000 for anti-rabbit or 1:5000 for anti-mouse in Tris-buffered saline (TBS) with 0.1% Tween®20 (Roth, Germany). The densitometry analysis from WBs was performed using the Image J 1.41o software (Wayne Rasband; National Institutes of Health, USA).

Isolation of mitochondria from HeLa cells and *in vitro* import assay

HeLa cells were cultured in DMEM supplemented with 10% FBS, 50 U/ml penicillin and 50 μg/ml streptomycin at 37°C under 5% CO_2. The cells in a 10 cm culture dish were washed with phosphate-buffered saline (PBS) and collected by centrifugation at 800*g* for 5 min. From here on, all steps were performed at 4°C. The collected cells were resuspended in buffer A (20 mM HEPES–KOH, 220 mM Mannitol, 70 mM sucrose, 1 mM EDTA, 2 mg/ml BSA and 0.5 mM PMSF, pH 7.6) and were homogenized by being passed 20 times through a 27-gauge needle, and then this mixture was centrifuged at 800*g* for 5 min. The supernatant fraction was centrifuged at 10 000*g* for 10 min to obtain the mitochondrial fraction. The mitochondria were resuspended in 1 ml buffer B (20 mM HEPES–KOH, 220 mM Mannitol, 70 mM sucrose, 0.5 mM PMSF, pH 7.6) and were centrifuged again at 10 000*g* for 10 min. This mitochondria pellet was then used for *in vitro* import assays.

Radiolabeled precursor proteins were synthesized by the TNT-coupled reticulocyte lysate system (Promega) in the presence of ^{35}S-methionine. The assay mixtures containing

precursor proteins and 25 μg mitochondria were incubated in 50 μl of import buffer (10 mM HEPES–KOH, 1 mM ATP, 20 mM sodium succinate, 5 mM NADPH, 0.5 mM magnesium acetate, 220 mM mannitol, 70 mM sucrose, 0.5 mM PMSF, pH 7.4) at 30°C for the indicated time in the absence (Fig. 3, lanes 2–5) or presence of CCCP (Fig. 3, lane 6, asterisk). To degrade non-imported proteins, samples were treated at the end of the reaction with proteinase K (100 μg/ml) for 30 min on ice. The mitochondria were then isolated by centrifugation and analyzed by SDS–PAGE followed by autoradiography.

Immunocytochemistry and immunofluorescence microscopy

For immunocytochemistry, HEK293 cells were seeded on collagen-coated slides and transiently transfected with either wt mortalin or mortalin variants or the corresponding empty vector. Forty-eight hours following transfection, cells were incubated for 15 min with 100 nM MitoTracker® Red CMX-Ros (Molecular Probes) at 37°C in a humidified 5% CO_2 atmosphere to visualize mitochondria via fluorescence microscopy. Then cells were washed with PBS, fixed with 10% (wt/vol.) paraformaldehyde (PFA) in PBS at room temperature for 15 min and permeabilized at −20°C with ice-cold methanol for 5 min. After washing, cells were incubated for 30 min in 10% (vol./vol.) FCS in PBS for blocking and subsequent incubation with rabbit V5 antibody (1:300) and visualization with a fluorescein isothiocyanate-conjugated anti-rabbit secondary antibody (1:5000; Dianova, Germany). Cell nuclei were stained with Hoechst 33342 (1:10 000; Molecular Probes). After a 3-fold wash step in PBS, the coverglass was mounted in Mowiol (Sigma). Mitochondrial localization of wt mortalin and mortalin variants was investigated using an epifluorescence microscope (Axioplan 2, Zeiss, Germany) with an ApoTome technique. Three slices with intervals between 0.230 and 0.280 μm were taken and the series of pictures were saved uncompressed. To determine the degree of colocalization, images were loaded into AxioVision 4.6 software and evaluated accordingly (Zeiss).

Live cell imaging

Mitochondrial morphology was analyzed by live cell imaging. SH-SY5Y cells or human fibroblasts were cultured in Lab-TekHII chambered coverglasses (number 155382; Nalge Nunc International). Mitochondria of fibroblasts were stained with 200 nM MitoTracker® Green FM (Invitrogen). SH-SY5Y cells were cotransfected 4 h after seeding in coverglasses with Mito-DsRed plasmid and either wt mortalin or one of its variants (A476T, R126W, P509S) in the ratio 1:4 using HiPerFect transfection reagent (Qiagen, Hilden, Germany). Hoechst 33342 (Molecular Probes) was used to stain nuclei. Analysis of mitochondrial morphology was performed using an inverted Zeiss Axiovert microscope (Zeiss Plan-Apochromat 63×/1.4) with an incubation chamber temperatured at 37°C. Stacks of the images were taken with an AxioCamMRm camera (Zeiss) with distances between 0.240 and 0.300 μm per stack. For each image, seven stacks were taken. The series of images were saved uncompressed and analyzed with AxioVision software (Zeiss).

Analysis of mitochondrial morphology

Fluorescence microscopy images were optimized by adjusting the contrast and subsequently binarized by conversion to 8 bit images. After reduction of unspecific noise of the fluorescence signal, a spatial filter (convolution filter) as well as a threshold was applied to the images to define mitochondrial structures. Using Image J 1.41o software, every single mitochondrion of the investigated cells was marked to analyze morphological characteristics such as its area, perimeter, major and minor axes. On the basis of these parameters, the AR of a mitochondrion (AR; ratio between the major and the minor axes of the ellipse equivalent to the object) and its FF [$\text{perimeter}^2/(4\pi \times \text{area})$], consistent with the degree of branching, were calculated (58).

Assessment of mitochondrial parameters by FACS measurement

To monitor the production of intramitochondrial ROS, cells were incubated in a medium containing 5 μM MitoSOX® (Invitrogen) for 20 min and washed twice with PBS. MMP was measured after incubation in a medium containing 100 nM TMRE for 30 min and washed twice with PBS. For proteolytic stress conditions, cells were treated with 10 μM protease inhibitor MG-132 (Sigma-Aldrich, Germany) for 16 h before harvesting the cells. For each measurement, at least 30 000 cells were analyzed for the corresponding fluorescence on a CyAnTM ADP apparatus (DakoCytomation) using the 488 nm argon laser and emission through the PE filter (575 nm). All experiments were performed in duplicate and repeated at least three times.

RNA interference-mediated downregulation of mortalin and retransfection with wt mortalin or mortalin variants

Mortalin gene silencing was established by transfection of *mortalin* HP GenomeWide siRNA or chemically unmodified non-targeting control siRNA from Qiagen (Germany) into human cells. As an efficient knockdown of mortalin in SH-SY5Y cells was linked with substantial cell death, either by the use of siRNA or by shRNA lentiviral transduction particles, we chose HEK293 cells as an alternate human cell line.

For the analysis of MMP and ROS production in cells with knockdown of endogenous mortalin and subsequent rescue experiments, 200 000 HEK293 cells were seeded in a 12-well plate and cultured in a 5% CO_2 humidified atmosphere in DMEM containing 10% FCS, 1% penicillin and streptomycin. After 4–5 h, cells were transfected with 80 pmol of *mortalin* siRNA or non-targeting control siRNA using HiPerFect transfection reagent (Qiagen), leading to a reduction in mortalin protein of up to 58% in cells transfected with *mortalin* siRNA compared with control cells. For rescue experiments, 24 h after transfection with siRNA, cells were again transfected with 4 μg of DNA by using jetPEI transfection reagent according to the manufacturer's instructions (Peqlab Biotechnologie GmbH, Erlangen, Germany). Following 24 h, cells were analyzed via a FACS method to determine the MMP or levels of ROS production as described above. Downregulation

of mortalin and complementation efficiency were monitored by immunoblotting with the mortalin antibody.

Statistical analysis

Genetic data were evaluated for allele frequencies and genotype frequencies using the Genepop program as described previously (59).

Functional data were analyzed by a Student's *t*-test; all statistical tests were two-sided, and those with a *P*-value <0.05 were considered to be statistically significant. Data are expressed as means $\pm$ standard deviation (SD) or means $\pm$ standard error (SE) values.

SUPPLEMENTARY MATERIAL

Supplementary Material is available at *HMG* online.

ACKNOWLEDGEMENTS

We are grateful to Dr Radhika Puttagunta for valuable comments during the preparation of the manuscript.

Conflict of Interest statement. None declared.

FUNDING

This work was supported by grants from the German Research Council (DFG, KR2119/3-2 to R.K. and RA1028/4-1 to D.R.); the Federal Ministry for Education and Research (BMBF, NGFNplus; 01GS08134 to R.K. and O.R.); the Faculty of Medicine, University of Tübingen (Fortuene 1709-0-0 to R.K.) and from the charitable Hertie Foundation (PhD stipend award to L.F.B.). The KORA research platform (KORA: Cooperative Research in the Region of Augsburg; http://www.gsf.de/KORA) was initiated and financed by the Forschungszentrum für Umwelt und Gesundheit (GSF), which is funded by the German Federal Ministry of Education, Science, Research and Technology and by the State of Bavaria.

REFERENCES

1. Schiesling, C., Kieper, N., Seidel, K. and Kruger, R. (2008) Review: familial Parkinson's disease—genetics, clinical phenotype and neuropathology in relation to the common sporadic form of the disease. *Neuropathol. Appl. Neurobiol.*, **34**, 255–271.
2. Simon-Sanchez, J., Schulte, C., Bras, J.M., Sharma, M., Gibbs, J.R., Berg, D., Paisan-Ruiz, C., Lichtner, P., Scholz, S.W., Hernandez, D.G. *et al.* (2009) Genome-wide association study reveals genetic risk underlying Parkinson's disease. *Nat. Genet.*, **41**, 1308–1312.
3. Schapira, A.H. (1999) Mitochondria in the aetiology and pathogenesis of Parkinson's disease. *Parkinsonism Relat. Disord.*, **5**, 139–143.
4. Strauss, K.M., Martins, L.M., Plun-Favreau, H., Marx, F.P., Kautzmann, S., Berg, D., Gasser, T., Wszolek, Z., Muller, T., Bornemann, A. *et al.* (2005) Loss of function mutations in the gene encoding Omi/HtrA2 in Parkinson's disease. *Hum. Mol. Genet.*, **14**, 2099–2111.
5. Valente, E.M., Salvi, S., Ialongo, T., Marongiu, R., Elia, A.E., Caputo, V., Romito, L., Albanese, A., Dallapiccola, B. and Bentivoglio, A.R. (2004) PINK1 mutations are associated with sporadic early-onset parkinsonism. *Ann. Neurol.*, **56**, 336–341.
6. Valente, E.M., Abou-Sleiman, P.M., Caputo, V., Muqit, M.M., Harvey, K., Gispert, S., Ali, Z., Del Turco, D., Bentivoglio, A.R., Healy, D.G. *et al.* (2004) Hereditary early-onset Parkinson's disease caused by mutations in PINK1. *Science*, **304**, 1158–1160.
7. Bonifati, V., Rizzu, P., Squitieri, F., Krieger, E., Vanacore, N., van Swieten, J.C., Brice, A., van Duijn, C.M., Oostra, B., Meco, G. *et al.* (2003) DJ-1(PARK7), a novel gene for autosomal recessive, early onset parkinsonism. *Neurol. Sci.*, **24**, 159–160.
8. Canet-Aviles, R.M., Wilson, M.A., Miller, D.W., Ahmad, R., McLendon, C., Bandyopadhyay, S., Baptista, M.J., Ringe, D., Petsko, G.A. and Cookson, M.R. (2004) The Parkinson's disease protein DJ-1 is neuroprotective due to cysteine-sulfinic acid-driven mitochondrial localization. *Proc. Natl Acad. Sci. USA*, **101**, 9103–9108.
9. Junn, E., Jang, W.H., Zhao, X., Jeong, B.S. and Mouradian, M.M. (2009) Mitochondrial localization of DJ-1 leads to enhanced neuroprotection. *J. Neurosci. Res.*, **87**, 123–129.
10. Abou-Sleiman, P.M., Healy, D.G., Quinn, N., Lees, A.J. and Wood, N.W. (2003) The role of pathogenic DJ-1 mutations in Parkinson's disease. *Ann. Neurol.*, **54**, 283–286.
11. Bonifati, V., Rizzu, P., van Baren, M.J., Schaap, O., Breedveld, G.J., Krieger, E., Dekker, M.C., Squitieri, F., Ibanez, P., Joosse, M. *et al.* (2003) Mutations in the DJ-1 gene associated with autosomal recessive early-onset parkinsonism. *Science*, **299**, 256–259.
12. Li, H.M., Niki, T., Taira, T., Iguchi-Ariga, S.M. and Ariga, H. (2005) Association of DJ-1 with chaperones and enhanced association and colocalization with mitochondrial Hsp70 by oxidative stress. *Free Radic. Res.*, **39**, 1091–1099.
13. Jin, J., Li, G.J., Davis, J., Zhu, D., Wang, Y., Pan, C. and Zhang, J. (2007) Identification of novel proteins associated with both alpha-synuclein and DJ-1. *Mol. Cell. Proteomics*, **6**, 845–859.
14. Wadhwa, R., Pereira-Smith, O.M., Reddel, R.R., Sugimoto, Y., Mitsui, Y. and Kaul, S.C. (1995) Correlation between complementation group for immortality and the cellular distribution of mortalin. *Exp. Cell Res.*, **216**, 101–106.
15. Ran, Q., Wadhwa, R., Kawai, R., Kaul, S.C., Sifers, R.N., Bick, R.J., Smith, J.R. and Pereira-Smith, O.M. (2000) Extramitochondrial localization of mortalin/mthsp70/PBP74/GRP75. *Biochem. Biophys. Res. Commun.*, **275**, 174–179.
16. Webster, T.J., Naylor, D.J., Hartman, D.J., Hoj, P.B. and Hoogenraad, N.J. (1994) cDNA cloning and efficient mitochondrial import of pre-mtHSP70 from rat liver. *DNA Cell Biol.*, **13**, 1213–1220.
17. Rehling, P., Brandner, K. and Pfanner, N. (2004) Mitochondrial import and the twin-pore translocase. *Nat. Rev. Mol. Cell Biol.*, **5**, 519–530.
18. Schneider, H.C., Berthold, J., Bauer, M.F., Dietmeier, K., Guiard, B., Brunner, M. and Neupert, W. (1994) Mitochondrial Hsp70/MIM44 complex facilitates protein import. *Nature*, **371**, 768–774.
19. Brunner, M., Schneider, H.C., Lill, R. and Neupert, W. (1995) Dissection of protein translocation across the mitochondrial outer and inner membranes. *Cold Spring Harb. Symp. Quant. Biol.*, **60**, 619–627.
20. Deocaris, C.C., Kaul, S.C. and Wadhwa, R. (2008) From proliferative to neurological role of an hsp70 stress chaperone, mortalin. *Biogerontology*, **9**, 391–403.
21. Takano, S., Wadhwa, R., Yoshii, Y., Nose, T., Kaul, S.C. and Mitsui, Y. (1997) Elevated levels of mortalin expression in human brain tumors. *Exp. Cell Res.*, **237**, 38–45.
22. Jin, J., Hulette, C., Wang, Y., Zhang, T., Pan, C., Wadhwa, R. and Zhang, J. (2006) Proteomic identification of a stress protein, mortalin/mthsp70/GRP75: relevance to Parkinson disease. *Mol. Cell. Proteomics*, **5**, 1193–1204.
23. Liu, Y., Liu, W., Song, X.D. and Zuo, J. (2005) Effect of GRP75/mthsp70/PBP74/mortalin overexpression on intracellular ATP level, mitochondrial membrane potential and ROS accumulation following glucose deprivation in PC12 cells. *Mol. Cell. Biochem.*, **268**, 45–51.
24. Kimura, K., Tanaka, N., Nakamura, N., Takano, S. and Ohkuma, S. (2007) Knockdown of mitochondrial heat shock protein 70 promotes progeria-like phenotypes in *Caenorhabditis elegans*. *J. Biol. Chem.*, **282**, 5910–5918.
25. Hajnoczky, G. and Hoek, J.B. (2007) Cell signaling. Mitochondrial longevity pathways. *Science*, **315**, 607–609.
26. Thal, D.R., Del Tredici, K. and Braak, H. (2004) Neurodegeneration in normal brain aging and disease. *Sci. Aging Knowledge Environ.*, **2004**, pe26.

27. Soti, C. and Csermely, P. (2002) Chaperones and aging: role in neurodegeneration and in other civilizational diseases. *Neurochem. Int.*, **41**, 383–389.
28. Yokoyama, K., Fukumoto, K., Murakami, T., Harada, S., Hosono, R., Wadhwa, R., Mitsui, Y. and Ohkuma, S. (2002) Extended longevity of *Caenorhabditis elegans* by knocking in extra copies of hsp70F, a homolog of mot-2 (mortalin)/mthsp70/Grp75. *FEBS Lett.*, **516**, 53–57.
29. Kaul, S.C., Yaguchi, T., Taira, K., Reddel, R.R. and Wadhwa, R. (2003) Overexpressed mortalin (mot-2)/mthsp70/GRP75 and hTERT cooperate to extend the *in vitro* lifespan of human fibroblasts. *Exp. Cell Res.*, **286**, 96–101.
30. Jin, J., Meredith, G.E., Chen, L., Zhou, Y., Xu, J., Shie, F.S., Lockhart, P. and Zhang, J. (2005) Quantitative proteomic analysis of mitochondrial proteins: relevance to Lewy body formation and Parkinson's disease. *Brain Res. Mol. Brain Res.*, **134**, 119–138.
31. Kaul, S.C., Deocaris, C.C. and Wadhwa, R. (2007) Three faces of mortalin: a housekeeper, guardian and killer. *Exp. Gerontol.*, **42**, 263–274.
32. Yaguchi, T., Aida, S., Kaul, S.C. and Wadhwa, R. (2007) Involvement of mortalin in cellular senescence from the perspective of its mitochondrial import, chaperone, and oxidative stress management functions. *Ann. NY Acad. Sci.*, **1100**, 306–311.
33. Perkins, D.N., Pappin, D.J., Creasy, D.M. and Cottrell, J.S. (1999) Probability-based protein identification by searching sequence databases using mass spectrometry data. *Electrophoresis*, **20**, 3551–3567.
34. De Mena, L., Coto, E., Sanchez-Ferrero, E., Ribacoba, R., Guisasola, L.M., Salvador, C., Blazquez, M. and Alvarez, V. (2009) Mutational screening of the mortalin gene (HSPA9) in Parkinson's disease. *J. Neural Transm*, **116**, 1289–1293.
35. Berg, D., Schweitzer, K., Leitner, P., Zimprich, A., Lichtner, P., Belcredi, P., Brussel, T., Schulte, C., Maass, S. and Nagele, T. (2005) Type and frequency of mutations in the LRRK2 gene in familial and sporadic Parkinson's disease. *Brain*, **128**, 3000–3011.
36. Mandemakers, W., Morais, V.A. and De Strooper, B. (2007) A cell biological perspective on mitochondrial dysfunction in Parkinson disease and other neurodegenerative diseases. *J. Cell Sci.*, **120**, 1707–1716.
37. Narendra, D., Tanaka, A., Suen, D.F. and Youle, R.J. (2008) Parkin is recruited selectively to impaired mitochondria and promotes their autophagy. *J. Cell Biol.*, **183**, 795–803.
38. Exner, N., Treske, B., Paquet, D., Holmstrom, K., Schiesling, C., Gispert, S., Carballo-Carbajal, I., Berg, D., Hoepken, H.H., Gasser, T. *et al.* (2007) Loss-of-function of human PINK1 results in mitochondrial pathology and can be rescued by parkin. *J. Neurosci.*, **27**, 12413–12418.
39. Krebiehl, G., Ruckerbauer, S., Burbulla, L.F., Kieper, N., Maurer, B., Waak, J., Wolburg, H., Gizatullina, Z., Gellerich, F.N., Woitalla, D. *et al.* (2010) Reduced basal autophagy and impaired mitochondrial dynamics due to loss of Parkinson's disease-associated protein DJ-1. *PLoS ONE*, **5**, e9367.
40. Kieper, N., Holmstrom, K.M., Ciceri, D., Fiesel, F.C., Wolburg, H., Ziviani, E., Whitworth, A.J., Martins, L.M., Kahle, P.J. and Kruger, R. (2010) Modulation of mitochondrial function and morphology by interaction of Omi/HtrA2 with the mitochondrial fusion factor OPA1. *Exp. Cell Res.*, **316**, 1213–1224.
41. Slater, M.R. and Craig, E.A. (1987) Transcriptional regulation of an hsp70 heat shock gene in the yeast *Saccharomyces cerevisiae*. *Mol. Cell. Biol.*, **7**, 1906–1916.
42. Hicks, A.A., Petursson, H., Jonsson, T., Stefansson, H., Johannsdottir, H.S., Sainz, J., Frigge, M.L., Kong, A., Gulcher, J.R., Stefansson, K. *et al.* (2002) A susceptibility gene for late-onset idiopathic Parkinson's disease. *Ann. Neurol.*, **52**, 549–555.
43. Scott, W.K., Nance, M.A., Watts, R.L., Hubble, J.P., Koller, W.C., Lyons, K., Pahwa, R., Stern, M.B., Colcher, A., Hiner, B.C. *et al.* (2001) Complete genomic screen in Parkinson disease: evidence for multiple genes. *JAMA*, **286**, 2239–2244.
44. Pankratz, N., Nichols, W.C., Uniacke, S.K., Halter, C., Murrell, J., Rudolph, A., Shults, C.W., Conneally, P.M. and Foroud, T. (2003) Genome-wide linkage analysis and evidence of gene-by-gene interactions in a sample of 362 multiplex Parkinson disease families. *Hum. Mol. Genet.*, **12**, 2599–2608.
45. Martinez, M., Brice, A., Vaughan, J.R., Zimprich, A., Breteler, M.M., Meco, G., Filla, A., Farrer, M.J., Betard, C., Hardy, J. *et al.* (2004) Genome-wide scan linkage analysis for Parkinson's disease: the European genetic study of Parkinson's disease. *J. Med. Genet.*, **41**, 900–907.
46. Deocaris, C.C., Yamasaki, K., Kaul, S.C. and Wadhwa, R. (2006) Structural and functional differences between mouse mot-1 and mot-2 proteins that differ in two amino acids. *Ann. NY Acad. Sci.*, **1067**, 220–223.
47. Liang, C.L., Wang, T.T., Luby-Phelps, K. and German, D.C. (2007) Mitochondria mass is low in mouse substantia nigra dopamine neurons: implications for Parkinson's disease. *Exp. Neurol.*, **203**, 370–380.
48. Radke, S., Chander, H., Schafer, P., Meiss, G., Kruger, R., Schulz, J.B. and Germain, D. (2008) Mitochondrial protein quality control by the proteasome involves ubiquitination and the protease Omi. *J. Biol. Chem.*, **283**, 12681–12685.
49. Deocaris, C.C., Kaul, S.C. and Wadhwa, R. (2006) On the brotherhood of the mitochondrial chaperones mortalin and heat shock protein 60. *Cell Stress Chaperones*, **11**, 116–128.
50. Wagner, I., Arlt, H., van Dyck, L., Langer, T. and Neupert, W. (1994) Molecular chaperones cooperate with PIM1 protease in the degradation of misfolded proteins in mitochondria. *EMBO J.*, **13**, 5135–5145.
51. Sanjuan Szklarz, L.K., Guiard, B., Rissler, M., Wiedemann, N., Kozjak, V., van der Laan, M., Lohaus, C., Marcus, K., Meyer, H.E., Chacinska, A. *et al.* (2005) Inactivation of the mitochondrial heat shock protein zim17 leads to aggregation of matrix hsp70s followed by pleiotropic effects on morphology and protein biogenesis. *J. Mol. Biol.*, **351**, 206–218.
52. Kawai, A., Nishikawa, S., Hirata, A. and Endo, T. (2001) Loss of the mitochondrial Hsp70 functions causes aggregation of mitochondria in yeast cells. *J. Cell Sci.*, **114**, 3565–3574.
53. Shi, M., Jin, J., Wang, Y., Beyer, R.P., Kitsou, E., Albin, R.L., Gearing, M., Pan, C. and Zhang, J. (2008) Mortalin: a protein associated with progression of Parkinson disease? *J. Neuropathol. Exp. Neurol.*, **67**, 117–124.
54. Gibb, W.R. and Lees, A.J. (1988) A comparison of clinical and pathological features of young- and old-onset Parkinson's disease. *Neurology*, **38**, 1402–1406.
55. Liu, Y., Lamkemeyer, T., Jakob, A., Mi, G., Zhang, F., Nordheim, A. and Hochholdinger, F. (2006) Comparative proteome analyses of maize (*Zea mays* L.) primary roots prior to lateral root initiation reveal differential protein expression in the lateral root initiation mutant rum1. *Proteomics*, **6**, 4300–4308.
56. Kohlbacher, O., Reinert, K., Gropl, C., Lange, E., Pfeifer, N., Schulz-Trieglaff, O. and Sturm, M. (2007) TOPP—the OpenMS proteomics pipeline. *Bioinformatics*, **23**, e191–e197.
57. Sturm, M., Bertsch, A., Gropl, C., Hildebrandt, A., Hussong, R., Lange, E., Pfeifer, N., Schulz-Trieglaff, O., Zerck, A., Reinert, K. *et al.* (2008) OpenMS—an open-source software framework for mass spectrometry. *BMC Bioinformatics*, **9**, 163.
58. Koopman, W.J., Verkaart, S., Visch, H.J., van der Westhuizen, F.H., Murphy, M.P., van den Heuvel, L.W., Smeitink, J.A. and Willems, P.H. (2005) Inhibition of complex I of the electron transport chain causes $O2^{\cdot-}$-mediated mitochondrial outgrowth. *Am. J. Physiol. Cell Physiol.*, **288**, C1440–C1450.
59. Kruger, R., Hardt, C., Tschentscher, F., Jackel, S., Kuhn, W., Muller, T., Werner, J., Woitalla, D., Berg, D., Kuhnl, N. *et al.* (2000) Genetic analysis of immunomodulating factors in sporadic Parkinson's disease. *J. Neural. Transm.*, **107**, 553–562.